



HAL
open science

Neogene exhumation and relief evolution in the eastern Betics (SE Spain): insights from the Sierra de Gador

Marianne Janowski, Nicolas Loget, Cécile Gautheron, Jocelyn Barbarand, Nicolas Bellahsen, Jean van den Driessche, Julien Babault, Bertrand Meyer

► **To cite this version:**

Marianne Janowski, Nicolas Loget, Cécile Gautheron, Jocelyn Barbarand, Nicolas Bellahsen, et al.. Neogene exhumation and relief evolution in the eastern Betics (SE Spain): insights from the Sierra de Gador. *Terra Nova*, 2017, 29 (2), pp.91-97. 10.1111/ter.12252 . hal-01447798

HAL Id: hal-01447798

<https://hal.science/hal-01447798>

Submitted on 2 Feb 2017

HAL is a multi-disciplinary open access archive for the deposit and dissemination of scientific research documents, whether they are published or not. The documents may come from teaching and research institutions in France or abroad, or from public or private research centers.

L'archive ouverte pluridisciplinaire **HAL**, est destinée au dépôt et à la diffusion de documents scientifiques de niveau recherche, publiés ou non, émanant des établissements d'enseignement et de recherche français ou étrangers, des laboratoires publics ou privés.

1 **Neogene exhumation and relief evolution in the eastern Betics (SE Spain): insights from**
2 **the Sierra de Gador**

3

4 Marianne Janowski¹, Nicolas Loget¹, Cécile Gautheron², Jocelyn Barbarand², Nicolas
5 Bellahsen¹, Jean Van Den Driessche³, Julien Babault⁴ and Bertrand Meyer¹

6 ¹Sorbonne Universités, UPMC Univ Paris 06, CNRS, Institut des Sciences de la Terre de Paris
7 (ISTeP), F-75005, Paris, France, ²Géosciences Paris-Sud (GEOPS), Université Paris-Sud,
8 Orsay, France, ³Géosciences Rennes, Université Rennes-1, France, ⁴Departament de Geologia,
9 Universitat Autònoma de Barcelona, Spain

10

11

12 **Abstract**

13

14 The Betics are a key area to study an orogenic landscape disrupted by late-orogenic extension.
15 New low-temperature thermochronology (LTT) data (AHe and AFT) coupled with geomorphic
16 constraints in the Sierra de Gador (Alpujarride complex) are used to reconstruct the cooling
17 history and evolution of relief during the Neogene. We document three stages: (1) a fast cooling
18 event between 23 and 16 Ma associated with the well-known extensive tectonic exhumation of
19 the Alpujarride unit, (2) a period of slow cooling between 16 and 7.2 Ma related to a planation
20 event and (3) a post-7.2 Ma surface uplift associated with the inversion of the Alboran domain
21 undetected by LTT. The planation event followed by this late uplift can explain the occurrence
22 of inherited low-relief surfaces overlain by Tortonian-Messinian platform deposits at the top of
23 the range. Finally, we propose that the Sierra de Gador is a more transient landscape than the
24 nearby Sierra Nevada.

25

26 **Introduction**

27

28 Exhumation of rocks and topographic evolution are two parameters that are closely related in
29 orogenic systems (*e.g.* England and Molnar, 1990). In active orogenic wedges, uplift and
30 exhumation of accreted rocks are generally associated with a pattern of high-elevation and high-
31 relief topography (Willett and Brandon, 2002). Then, progressive removal of the lithospheric
32 root together with surface erosion or tectonic unroofing leads to topographic decrease in post-
33 orogenic settings. The final stage tends towards low-elevation and low-relief topographies
34 associated to low-temperature plateaus in cooling paths (Calvet *et al.*, 2015). The occurrence
35 of planar landforms at the top of mountain ranges illustrates a topographic transient stage linked
36 to a large-scale tectonic perturbation or local base-level changes during orogenic evolution (*e.g.*
37 Babault *et al.*, 2007; Calvet *et al.*, 2015). The Betics in southern Spain (Fig. 1) are an example
38 of such orogenic disruption (*e.g.* Platt and Vissers, 1989; Lonergan and White, 1997; Jolivet *et*
39 *al.*, 2008), where low-relief surfaces are described at the top of ranges (Farines *et al.*, 2015).
40 The Eocene-Oligocene mountain building is disrupted by an Oligocene-Miocene extensional
41 event associated with the collapse of the internal zones. Major detachments enabled the
42 exhumation of metamorphosed stacked nappes as the Alpujarride complex and the underlying
43 Nevado-Filabride complex (Fig. 1). The system has been inverted and the Betic crust shortened
44 since the Late Tortonian, as demonstrated by the folding of Miocene deposits (*e.g.* Weijermars
45 *et al.*, 1985; Sanz de Galdeano and Vera, 1992). Although the cooling event associated with the
46 Miocene extensional event is well known, the late story, related to the final extensive stage and
47 the following compressional event, remains poorly constrained, especially for the Alpujarride
48 domain. Yet, this is the main basement area where surface uplift and topographic building can
49 be constrained thanks to uplifted Miocene platform deposits (Braga *et al.*, 2003). This study is
50 focused on the Sierra de Gador, which forms the largest antiform of the Alpujarride domain and

51 is still covered by remnants of Miocene platform deposits overlying a smooth topography.
52 Thanks to low-temperature thermochronology (LTT) data (fission tracks and (U-Th)/He on
53 apatite), we show that the current topography is inherited from a Middle-Upper Miocene
54 planation event coeval with the late extensional stage of the eastern Betics. The post-Tortonian
55 regional inversion, characterized by a strong surface uplift, is undetected by LTT data,
56 suggesting that the Sierra de Gador topography is transient in nature.

57

58

59 **Geological setting**

60

61 The Betics are located at the western edge of the peri-Mediterranean alpine ranges and form the
62 northern part of the Betic-Rif arcuate mountain belt surrounding the Alboran Sea (Fig. 1). This
63 orogenic arc results from the Meso-Cenozoic convergence between Africa and Iberia. The Betic
64 ranges can be subdivided into non-metamorphic external zones and metamorphic internal
65 zones. The external zones are composed of folded and deformed sediments of the Iberian paleo-
66 margin thrust over the autochthonous Iberian platform, forming the Guadalquivir foreland
67 basin, which is filled by Neogene sediments (Michard *et al.*, 2002; Frizon de Lamotte *et al.*,
68 2004). The internal zones (or Alboran domain) are composed of a stack of three nappes of
69 different metamorphic grade; from bottom to top they are the Nevado-Filabride, the Alpujarride
70 and the Malaguide complexes. These nappes were accreted during the pre-Miocene collisional
71 stage and then mainly exhumed during a Miocene extensional event (Martínez-Martínez and
72 Azañón, 1997; Azañón and Crespo-Blanc, 2000). During this period, the development of low-
73 angle normal faults induced the separation of the three complexes, as observed currently. This
74 extensional stage within the internal zones is coeval with thrusting and shortening in the
75 external zones. This pattern can be explained by deep tectonic processes such as convective

76 removal, delamination or slab rollback (*e.g.* Calvert *et al.*, 2000). Lithospheric imaging and
77 volcanic data support a westward slab rollback model (Lonergan and White, 1997; Duggen *et*
78 *al.*, 2004; Faccenna *et al.*, 2004; Spakman and Wortel, 2004). The extensional stage induced a
79 major thinning of the Alboran domain and resulted in the formation of marine sedimentary
80 basins including the Alboran basin (Sanz de Galdeano and Vera, 1992; Comas *et al.*, 1999).
81 Since the Late Tortonian, the internal zones have undergone N-S to NW-SE compression,
82 inducing large-scale folding and the emergence of a part of their overlying marine basins
83 (Weijermars, 1985; Comas *et al.*, 1999; Marín-Lechado *et al.*, 2007; Iribarren *et al.*, 2009).

84

85

86 **Exhumation and topographic features of the eastern Betics**

87

88 The topography of the Betics can be described by a succession of ranges separated by
89 depressions where Miocene marine and continental basins are preserved (Fig. 1). The elevations
90 of these ranges reach more than 3000 m in the Sierra Nevada and more than 2000 m in the
91 Sierra de Gador. These ranges correspond to large E-W antiforms of the exhumed Alboran
92 domain. The relief of the ranges corresponds to incised topographies, such as in the Sierra
93 Nevada (Pérez-Peña *et al.*, 2010), or, more remarkably, to low-relief surfaces at the top of
94 ranges, as in Sierra de Gador (Figs. 2 et 3; Farines *et al.*, 2015). In the Sierra Nevada, composed
95 of Nevado-Filabride units, AFT and AHe ages range from 2.7 ± 0.6 to 10.5 ± 0.9 Ma (Fig. 2)
96 and from 6.2 ± 0.4 to 8.8 ± 0.5 Ma respectively (Johnson *et al.*, 1997; Reinhardt *et al.*, 2007;
97 Clark and Dempster, 2009; Vázquez *et al.*, 2011). AFT ages show a westward rejuvenation
98 interpreted as the consequence of the top-to-the-WSW extension along the tectonic contact
99 between the Nevado-Filabride and the Alpujarride complexes (Johnson, 1997; Johnson *et al.*,
100 1997). Thermal history indicates a rapid cooling (660 to 60°C) between ~16.5 and 6-8 Ma,

101 followed by a slow cooling to surface conditions, reached at around 3-5 Ma (Vázquez *et al.*,
102 2011). Very young AFT ages in western Sierra Nevada are interpreted as the result of a fold
103 core's late extensional collapse (Reinhardt *et al.* 2007). In the Sierra de Gador, composed of
104 Alpujarride units, no thermochronological data are available except in the western valley where
105 AFT ages of ~16 Ma have been reported (Fig. 2, samples PB365 and PB367 from Platt *et al.*,
106 2005). A coupling with Ar/Ar data (~25 Ma) suggests a rapid cooling event during the early
107 Miocene (Fig. 2, samples PB369 and PB533 from Platt *et al.*, 2005). The timing of the final
108 exhumation of the Sierra de Gador cannot be determined due to the lack of LTT data (such as
109 AHe). Remnants of inner-platform calcarenites deposited around 7.2 Ma (uppermost Tortonian-
110 lowermost Messinian) now at high elevation (up to 1600 m) indicate that an important surface
111 uplift has occurred since the end of the Tortonian (Braga *et al.*, 2003). This uplift results from
112 the combination of a small-wavelength uplift induced by folding and a greater one induced by
113 regional dynamic topography (Marín-Lechado *et al.*, 2007; Garcia-Castellanos and Villaseñor,
114 2011). These deposits lie on a low-relief topography (<250 m; Figs. 2 and 3), and the whole
115 area has been affected by a Late Tortonian-Early Messinian planation event (Farines *et al.*,
116 2015). The low-relief summits now observed in the Sierra de Gador can be explained by this
117 polygenic erosional process. Finally, although a Late Miocene-Early Pliocene exhumation in
118 the Sierra Nevada associated with the post-Tortonian folding event has been proposed (Vázquez
119 *et al.*, 2011), its equivalent has not been described in the Sierra de Gador.

120

121

122 **LT thermochronology and thermal modelling**

123

124 Eleven samples were initially collected for LT thermochronology analysis in the Alpujarride
125 complex (sampled in quartzite and phyllite areas) and four AHe datings were performed (Ga-

126 04, Ga-07, Ga-09 and Ga-1; Fig. 4 and Supporting Information). In this area, the scarcity of
127 apatites and their low uranium content (Johnson *et al.*, 1997; Platt *et al.*, 2005) led us to select
128 Ga-04 (nearest sample from Tortonian calcarenites) for AFT dating to determine a Sierra de
129 Gador cooling path (Fig. 4 and Supporting Information). Alpha-ejection-corrected AHe ages
130 show apparent cooling AHe ages ranging from 9.2 ± 0.7 to 200 ± 16.2 Ma with no age-elevation
131 relationship but a negative correlation between eU content and AHe apparent ages (Fig. 4).
132 Spiegel *et al.* (2009) and Gautheron *et al.* (2012) have shown that the age-eU negative
133 correlation can be interpreted as the result of He implantation from the surrounding material
134 richer in U and Th than most of apatites. Murray *et al.* (2014) show also that implantation can
135 affect AHe age even for a low U-content of the surrounding medium. Following this
136 implantation model, the implantation-free age (or 'true' age) corresponds to the apparent age
137 of the single grain with the highest eU content, which, in our study, corresponds to a AHe 'true'
138 age of 9.2 ± 0.7 Ma (Fig. 4; Supporting Information). Sample Ga-04 shows an AFT central age
139 of 16 ± 2 Ma corresponding to the AFT ages proposed for the Alpujarride complex in the
140 western valley (PB365 dated at 16.1 ± 1.5 Ma and PB367 dated at 16.5 ± 1.5 Ma; Platt *et al.*,
141 2005; Figs. 2 and 4). We propose a common exhumation history for the Sierra de Gador and its
142 western valley on the basis of the similar AFT ages without age-elevation correlation (Fig. 4),
143 and the similar levels of erosion of the Alpujarride units partially covered by Tortonian
144 sediments.

145 Thermal modelling was performed using QTQt software (Gallagher, 2012) to infer the Neogene
146 cooling history of the Sierra de Gador. In addition to the new AHe data (age of 9.2 ± 0.7 Ma)
147 and AFT age (16 ± 2 Ma), published AFT (PB365 dated at 16.1 ± 1.5 Ma; PB367 dated at 16.5
148 ± 1.5 Ma) and muscovite Ar/Ar (PB369 dated at 22.7 ± 0.8 Ma; PB533 dated at 26.0 ± 1.9 Ma)
149 data for the Alpujarride complex were used as a vertical profile (Platt *et al.*, 2005; Fig. 2). The
150 resulting model (Fig. 5A) shows a polyphase thermal story with three clear stages: (1) a first

151 stage of very fast cooling between 23 and 16 Ma ($\sim 45^{\circ}\text{C}/\text{Ma}$); (2) a second stage of strong
152 cooling slowing down between 16 and 7.2 Ma ($\sim 11.5^{\circ}\text{C}/\text{Ma}$); and (3) a third stage of near-
153 surface conditions since 7.2 Ma without late reheating.

154

155

156 **Discussion and conclusions**

157

158 Our results show an unsteady exhumation since the early Miocene. To infer exhumation rates,
159 we used a mean geothermal gradient of $49 \pm 11^{\circ}\text{C}/\text{km}$ following the range published for the
160 Alpujarride complex exhumation (Argles *et al.*, 1999; Azañón and Crespo-Blanc, 2000).
161 During the first cooling stage (23-16 Ma), rocks were exhumed at a rate of ~ 0.9 mm/yr. Such a
162 fast cooling event has been widely described for the Alpujarride complex (Sosson *et al.*, 1998;
163 Comas *et al.*, 1999; Platt *et al.*, 2005) and interpreted as a late stage of post-orogenic thinning
164 leading to the exhumation of a previously deeply buried metamorphic alpine-type nappe-stack
165 (Fig. 5B). Then, during the second cooling stage (16-7.2 Ma), Alpujarride rocks from the Sierra
166 de Gador kept exhuming but at a lower rate of ~ 0.2 mm/yr, whereas the Nevado-Filabride units
167 located further north, exhumed at a higher rate of ~ 1 mm/y (Johnson *et al.*, 1997; Vázquez *et*
168 *al.*, 2011) (Fig. 5A). During the 16-7.2 period, the Alpujarride topography decreased toward
169 sea-level, whereas the Nevado-Filabride unit likely remained in a higher position, as suggested
170 by the current difference in crustal thickness (Diaz *et al.*, 2016; Fig. 5B). These two units are
171 separated by the Alpujarras corridor, which is mainly filled by Serravallian and Tortonian
172 sediments eroded from Alpujarride-Malaguide and Nevado-Filabride units respectively
173 (Rodríguez Fernández *et al.*, 1990; Farines *et al.*, 2015). However, the Sierra de Gador summit
174 surfaces seem to have been formed during pre-Tortonian times (Farines *et al.*, 2015). According
175 to our thermochronological results coupled with these surface and stratigraphic constraints, we

176 propose that the current low relief at the top of the Sierra de Gador started to be shaped 16 Ma
177 ago (Fig. 5). Indeed, an important decrease in the exhumation rate coeval with topography
178 decrease toward sea-level strongly suggests a levelling process. Some works have shown that
179 an important decrease in the cooling rate tending towards a low-temperature plateau is often
180 associated with planation processes, as in the Sierra de los Filabres (Calvet *et al.*, 2015; Farines
181 *et al.*, 2015). At 7.2 Ma, surface temperatures were reached (Fig. 5A) and the low topography
182 was then flooded and reworked by the sea, and inner-platform calcarenites were deposited (Fig.
183 5B). Low-relief summits, described at a larger scale in the Betics, can be due to Miocene erosion
184 events, as described in the Sierra de Gador (Farines *et al.*, 2015). After 7.2 Ma, the Sierra de
185 Gador was uplifted and the Alpujarride rocks have remained at surface temperature conditions.
186 This non-resetting of thermochronometers implies that the upper Tortonian cover was thin, in
187 good agreement with the 100-200 m thickness depicted in the preserved Poniente basin further
188 south (Pedrera *et al.*, 2015). We also cannot distinguish exhumation of rocks after 7.2 Ma,
189 contrary to what has been described for the Sierra Nevada (Johnson *et al.*, 1997; Reinhardt *et*
190 *al.*, 2007; Vázquez *et al.*, 2011). In particular, some authors have proposed a stage of accelerated
191 exhumation around 4-5 Ma linked to a denudation affecting the western Sierra Nevada (Johnson
192 *et al.*, 1997; Reinhardt *et al.*, 2007). This denudation could be the result of focused crustal
193 folding accompanied by gravity sliding along surface detachments (Reinhardt *et al.*, 2007).
194 Marín-Lechado *et al.*, (2007) proposed that the elevation decrease of the ranges southward is
195 related to a decrease of the folding amplitude. Moreover, the dynamic topographic effect
196 described in the eastern Betics (García-Castellanos and Villaseñor, 2011) induces a
197 superimposed uplift signal, which may be higher in the Sierra Nevada as it is located directly
198 above the Iberian slab tear (Mancilla *et al.*, 2015). One can suppose that the resulting uplift in
199 the Sierra de Gador was not high enough to induce important denudation after 7.2 Ma. The
200 degree of fluvial erosion indicates roughly whether there has been equilibrium between uplift

201 and erosion of landscapes over the last million years (*e.g.*, Whipple, 2001). The presence of
202 minimally dissected summit surfaces in the Sierra de Gador argues for a transient state of the
203 range's topography, whereas equilibrium seems to have been reached for the Sierra Nevada
204 (Azañón *et al.*, 2015). This difference could be explained either by a later uplift stage of the
205 Sierra de Gador and/or by the resetting of the topography due to the Tortonian marine
206 transgression. Indeed, the absence of initial topography increases the landscape response time
207 following an uplift (Lague *et al.*, 2003). The current landscape of the Sierra de Gador results
208 from inherited low relief, which was mainly initiated during Late Miocene, then uplifted and
209 slightly dissected since 7.2 Ma. Finally, the topography of this range appears to be transient,
210 indicating that transient landforms can develop and persist for several Myr during orogenic
211 evolution.

212

213

214 **Acknowledgements**

215

216 The authors thank editor J. Braun, associate editor C. Spiegel, reviewers T. Dempster, U.
217 Glasmacher and an anonymous reviewer for their constructive comments. We also thank
218 Rosella Pinna-Jaume for the U-Th chemistry preparation. Kerry Gallagher is thanked for
219 assistance with the setup of QTQt runs. M.J., N.L., J.VDD. and J. Babault collected the samples.
220 M.J., C.G and J. Barbarand performed LTT analyses. All authors contributed to writing the
221 paper. This work benefitted from the support of the French INSU-CNRS project Action-
222 Marges.

223

224

225

226 **References**

227

228 Argles, T.W., Platt, J.P., Waters, D.J., 1999. Attenuation and excision of a crustal section during
229 extensional exhumation: the Carratraca Massif, Betic Cordillera, southern Spain. *J.*
230 *Geol. Soc.*, **156**, 149–162.

231 Azañón, J.-M., Crespo-Blanc, A., 2000. Exhumation during a continental collision inferred
232 from the tectonometamorphic evolution of the Alpujarride Complex in the central Betics
233 (Alboran Domain, SE Spain). *Tectonics*, **19**, 549–565.

234 Azañón, J.M., Galve, J.P., Pérez-Peña, J.V., Giaconia, F., Carvajal, R., Booth-Rea, G., Jabaloy,
235 A., Vázquez, M., Azor, A., Roldán, F.J., 2015. Relief and drainage evolution during the
236 exhumation of the Sierra Nevada (SE Spain): Is denudation keeping pace with uplift?
237 *Tectonophysics*, **663**, 19–32.

238 Babault, J., Bonnet, S., Driessche, J.V.D., Crave, A., 2007. High elevation of low-relief surfaces
239 in mountain belts: does it equate to post-orogenic surface uplift? *Terra Nova*, **19**, 272–
240 277.

241 Braga, J.C., Martín, J.M., Quesada, C., 2003. Patterns and average rates of late Neogene-Recent
242 uplift of the Betic Cordillera, SE Spain. *Geomorphology*, **50**, 3–26.

243 Calvert, A., Sandvol, E., Seber, D., Barazangi, M., Roecker, S., Mourabit, T., Vidal, F.,
244 Alguacil, G., Jabour, N., 2000. Geodynamic evolution of the lithosphere and upper
245 mantle beneath the Alboran region of the western Mediterranean: Constraints from
246 travel time tomography. *J. Geophys. Res. Solid Earth*, **105**, 10871–10898.

247 Calvet, M., Gunnell, Y., Farines, B., 2015. Flat-topped mountain ranges: Their global
248 distribution and value for understanding the evolution of mountain topography.
249 *Geomorphology*, **241**, 255–291.

250 Clark, S.J.P., Dempster, T.J., 2009. The record of tectonic denudation and erosion in an
251 emerging orogen: an apatite fission-track study of the Sierra Nevada, southern Spain. *J.*
252 *Geol. Soc.*, **166**, 87–100.

253 Comas, M.C., Platt, J.P., Soto, J.I., Watts, A.B., 1999. 44. The origin and tectonic history of the
254 Alboran Basin: insights from Leg 161 results. In: *Proceedings of the Ocean Drilling*
255 *Program scientific results*, **161**, 555–580.

256 Diaz, J., Gallart, J., Carbonell, R., 2016. Moho topography beneath the Iberian-Western
257 Mediterranean region mapped from controlled-source and natural seismicity surveys.
258 *Tectonophysics*, **692**, 74-85.

259 Duggen, S., Hoernle, K., van den Bogaard, P., Harris, C., 2004. Magmatic evolution of the
260 Alboran region: The role of subduction in forming the western Mediterranean and
261 causing the Messinian Salinity Crisis. *Earth Planet Sci. Lett.*, **218**, 91–108.

262 England, P., Molnar, P., 1990. Surface uplift, uplift of rocks, and exhumation of rocks. *Geology*,
263 **18**, 1173–1177.

264 Faccenna, C., Piromallo, C., Crespo-Blanc, A., Jolivet, L., Rossetti, F., 2004. Lateral slab
265 deformation and the origin of the western Mediterranean arcs. *Tectonics*, **23**, 1–21.

266 Farines, B., Calvet, M., Gunnell, Y., 2015. The summit erosion surfaces of the inner Betic
267 Cordillera: Their value as tools for reconstructing the chronology of topographic growth
268 in southern Spain. *Geomorphology*, **233**, 92–111.

269 Frizon de Lamotte, D., Crespo-Blanc, A., Saint-Bézar, B., Comas, M., Fernandez, M., Zeyen,
270 H., Ayarza, P., Robert-Charrue, C., Chalouan, A., Zizi, M., 2004. TRANSMED
271 Transect I: Iberian Meseta–Guadalquivir Basin–Betic Cordillera–Alboran Sea–Rif–
272 Moroccan Meseta–High Atlas–Sahara Platform. In: *TRANSMED Atlas Mediterr. Reg.*
273 *Crust Mantle* (Cavazza, W., Roure, F.M., Spakman, W., Stampfli, G.M., Ziegler, P.A,
274 eds.) Springer.

275 Gallagher, K., 2012. Transdimensional inverse thermal history modeling for quantitative
276 thermochronology. *J. Geophys. Res.*, **117**, 1–16.

277 Garcia-Castellanos, D., Villaseñor, A., 2011. Messinian salinity crisis regulated by competing
278 tectonics and erosion at the Gibraltar arc. *Nature*, **480**, 359–363.

279 Gautheron, C., Tassan-Got, L., Ketcham, R.A., Dobson, K.J., 2012. Accounting for long alpha-
280 particle stopping distances in (U-Th-Sm)/He geochronology: 3D modeling of diffusion,
281 zoning, implantation, and abrasion. *Geochim. Cosmochim. Acta*, **96**, 44–56.

282 Iribarren, L., Vergés, J., Fernández, M., 2009. Sediment supply from the Betic–Rif orogen to
283 basins through Neogene. *Tectonophysics*, **475**, 68–84.

284 Johnson, C., 1997. Resolving denudational histories in orogenic belts with apatite fission-track
285 thermochronology and structural data: An example from southern Spain. *Geology*, **25**,
286 623–626.

287 Johnson, C., Harbury, N., Hurford, A.J., 1997. The role of extension in the Miocene denudation
288 of the Nevado-Filabride Complex, Betic Cordillera (SE Spain). *Tectonics*, **16**, 189–204.

289 Jolivet, L., Augier, R., Faccenna, C., Negro, F., Rimmelé, G., Agard, P., Robin, C., Rossetti,
290 F., Crespo-Blanc, A., 2008. Subduction, convergence and the mode of backarc
291 extension in the Mediterranean region. *Bull. Société Géologique Fr.*, **179**, 525–550.

292 Lague, D., Crave, A. and Davy, P., 2003. Laboratory experiments simulating the geomorphic
293 response to tectonic uplift. *J. Geophys. Res.*, **108**, 1-20.

294 Lonergan, L., White, N., 1997. Origin of the Betic-Rif mountain belt. *Tectonics*, **16**, 504–522.

295 Mancilla, F. de L., Booth-Rea, G., Stich, D., Pérez-Peña, J.V., Morales, J., Azañón, J.M.,
296 Martín, R., Giaconia, F., 2015. Slab rupture and delamination under the Betics and Rif
297 constrained from receiver functions. *Tectonophysics*, **663**, 225–237.

298 Marín-Lechado, C., Galindo-Zaldívar, J., Rodríguez-Fernández, L.R., Pedrera, A., 2007.
299 Mountain Front Development by Folding and Crustal Thickening in the Internal Zone
300 of the Betic Cordillera-Alboran Sea Boundary. *Pure Appl. Geophys.*, **164**, 1–21.

301 Martínez-Martínez, J.M., Azañón, J.M., 1997. Mode of extensional tectonics in the
302 southeastern Betics (SE Spain): Implications for the tectonic evolution of the peri-
303 Alborán orogenic system. *Tectonics*, **16**, 205–225.

304 Michard, A., Chalouan, A., Feinberg, H., Goffé, B., Montigny, R., 2002. How does the Alpine
305 belt end between Spain and Morocco? *Bull. Société Géologique Fr.*, **173**, 3–15.

306 Murray, K.E., Orme, D.A., Reiners, P.W., 2014. Effects of U–Th-rich grain boundary phases
307 on apatite helium ages. *Chem. Geol.*, **390**, 135–151.

308 Pedrera, A., Marín-Lechado, C., Galindo-Zaldívar, J., Lobo, F.J., 2015. Smooth folds favoring
309 gypsum precipitation in the Messinian Poniente marginal basin (Western
310 Mediterranean). *Tectonophysics*, **663**, 48–61.

311 Pérez-Peña, J.V., Azor, A., Azañón, J.M., Keller, E.A., 2010. Active tectonics in the Sierra
312 Nevada (Betic Cordillera, SE Spain): Insights from geomorphic indexes and drainage
313 pattern analysis. *Geomorphology*, **119**, 74–87.

314 Platt, J.P., Kelley, S.P., Carter, A., Orozco, M., 2005. Timing of tectonic events in the
315 Alpujarride Complex, Betic Cordillera, southern Spain. *J. Geol. Soc.*, **162**, 451–462.

316 Platt, J.P., Vissers, R.L.M., 1989. Extensional collapse of thickened continental lithosphere: A
317 working hypothesis for the Alboran Sea and Gibraltar arc. *Geology*, **17**, 540–543.

318 Reinhardt, L.J., Dempster, T.J., Shroder, J.F., Persano, C., 2007. Tectonic denudation and
319 topographic development in the Spanish Sierra Nevada. *Tectonics*, **26**, 1–14.

320 Rodríguez Fernández, J., Sanz de Galdeano, C., Serrano, F., 1990. Le couloir des Alpujarras.
321 In: C. Montenat (Ed.), *Les bassins néogènes du domaine bétique oriental (Espagne)*:

322 *tectonique et sédimentation dans un couloir de décrochement. Etude régionale* (pp. 12-
323 13). Paris, France: Institut géologique Albert de Lapparent.

324 Sanz De Galdeano, C.S., Vera, J.A., 1992. Stratigraphic record and palaeogeographical context
325 of the Neogene basins in the Betic Cordillera, Spain. *Basin Res.*, **4**, 21–35.

326 Sosson, M., Morillon, A.-C., Bourgois, J., Féraud, G., Poupeau, G., and Saint-Marc, P., 1998.
327 Late exhumation stages of the Alpujarride Complex (western Betic Cordilleras, Spain):
328 new thermochronological and structural data on Los Reales and Ojen nappes.
329 *Tectonophysics*, **285**, 253–273.

330 Spakman, W., Wortel, R., 2004. A tomographic view on western Mediterranean geodynamics.
331 In: *The TRANSMED Atlas. The Mediterranean region from crust to mantle* Springer,
332 31–52.

333 Spiegel, C., Kohn, B., Belton, D., Berner, Z., Gleadow, A., 2009. Apatite (U-Th-Sm)/He
334 thermochronology of rapidly cooled samples: The effect of He implantation. *Earth*
335 *Planet Sci. Lett.*, **285**, 105–114.

336 Vázquez, M., Jabaloy, A., Barbero, L., Stuart, F.M., 2011. Deciphering tectonic- and erosion-
337 driven exhumation of the Nevado-Filábride Complex (Betic Cordillera, Southern Spain)
338 by low-temperature thermochronology: deciphering tectonic- and erosion-driven
339 exhumation. *Terra Nova*, **23**, 257–263.

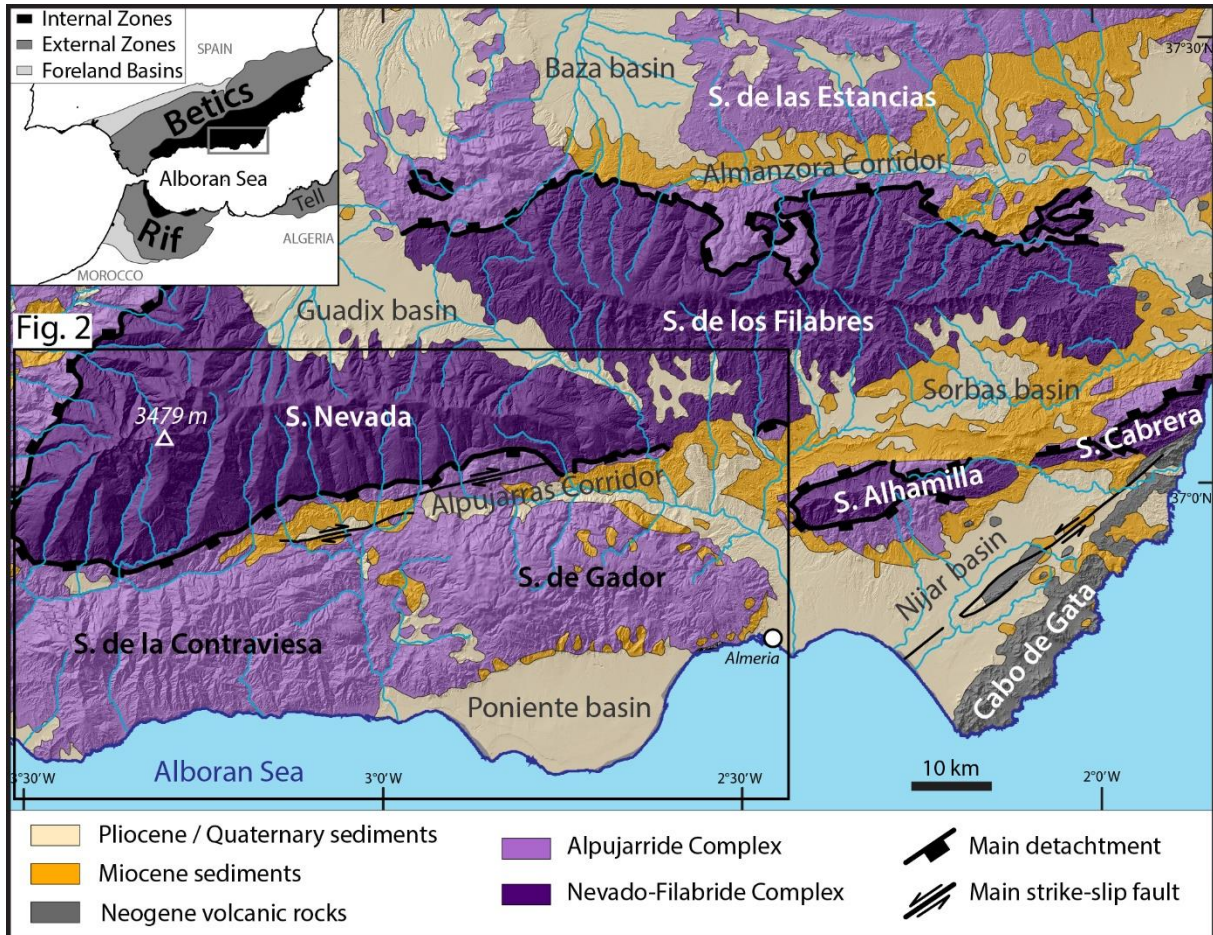
340 Weijermars, R., 1985. Uplift and subsidence history of the Alboran Basin and a profile of the
341 Alboran Diapir (W-Mediterranean). *Geologie en Mijnbouw*, **64**, 397–411.

342 Weijermars, R., Roep, Th., Van den Eeckhout, B., Postma, R., and Kleverlaan, K., 1985. Uplift
343 history of a Betic fold nappe inferred from Neogene-Quaternary sedimentation and
344 tectonics (in the Sierra Alhamilla and Almeria, Sorbas and Tabernas basins of the Betic
345 Cordilleras, SE Spain). *Geologie en Mijnbouw*, **64**, 397–411.

- 346 Whipple, K.X., 2001. Fluvial landscape response time: how plausible is steady-state
347 denudation? *Am. J. Sci.*, **301**, 313–325.
- 348 Willett, S.D., Brandon, M.T., 2002. On steady states in mountain belts. *Geology*, **30**, 175–178.

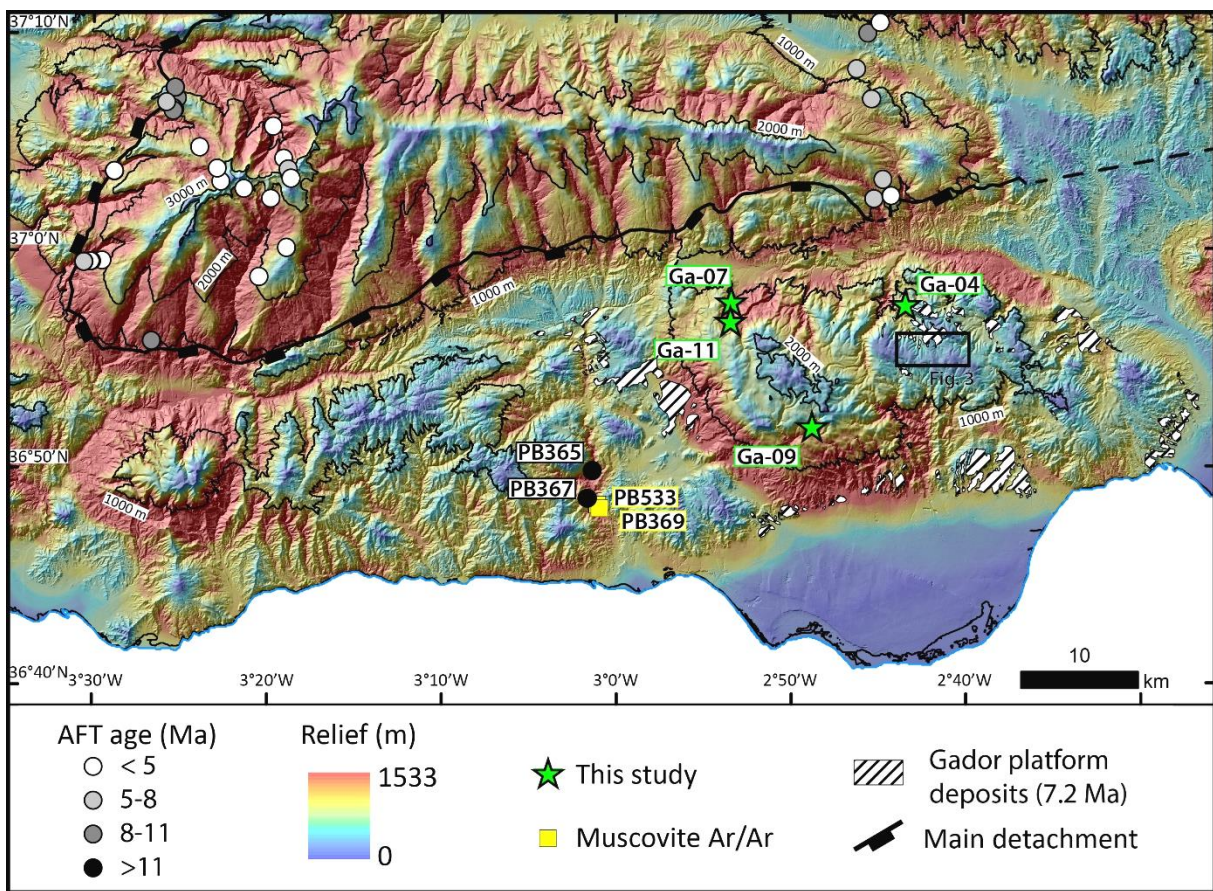
349 **Figure 1.** Simplified geological map of the eastern Betics showing the main tectonic units and
 350 Neogene basins. Inset shows the main tectonic domains of the peri-Alboran orogenic system in
 351 western Mediterranean.

352
 353



354
 355

356 **Figure 2.** Shaded relief map of the eastern Betics showing the locations of the
 357 thermochronological samples and sedimentary markers used in this study. Elevation contours
 358 are plotted every 1000 m. Relief map was compiled with a 3 km-radius sliding window. Note
 359 the widespread presence of low relief (<250 m) extracted at high elevations (>1000 m) at the
 360 top of the Sierra de Gador. Samples plotted are from this study and from published data
 361 (Johnson *et al.*, 1997; Platt *et al.*, 2005; Reinhardt *et al.*, 2007; Clark and Dempster, 2009;
 362 Vázquez *et al.*, 2011)



363

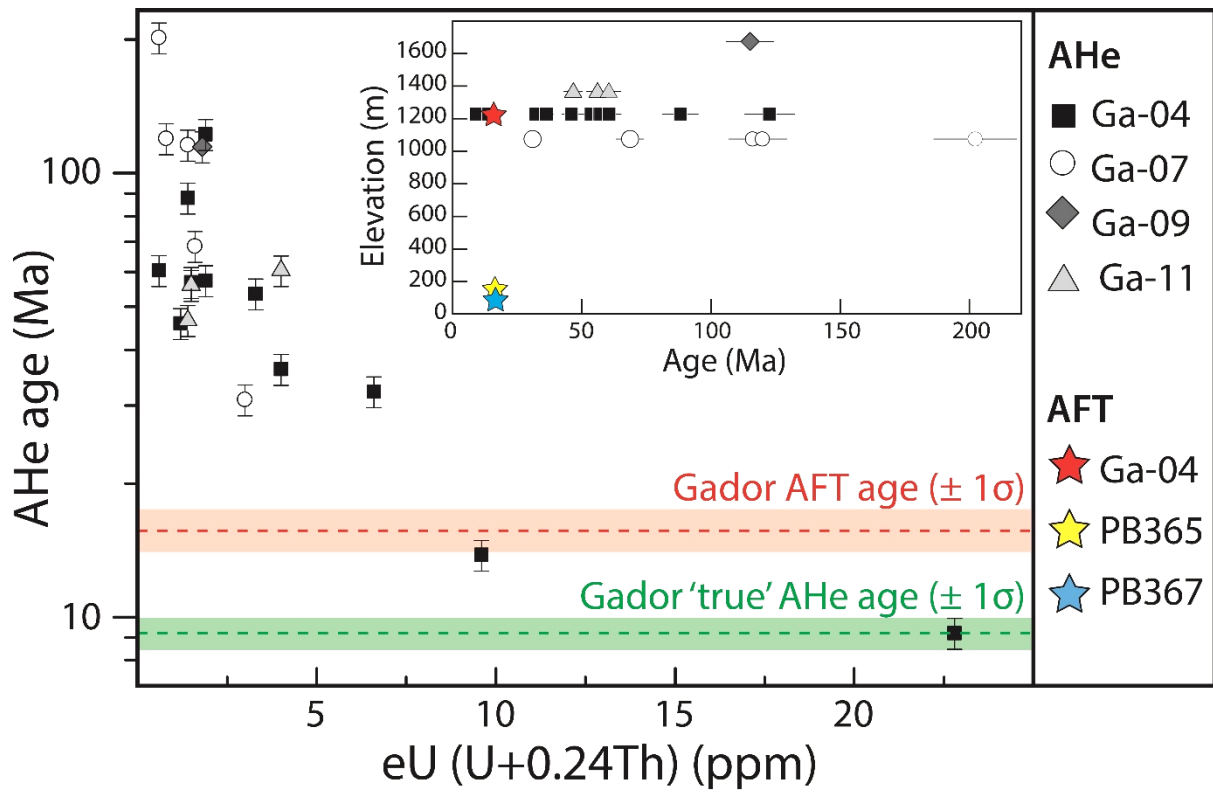
364 **Figure 3.** Photograph (looking north) showing low-relief surfaces overlain by thin calcarenite
365 deposits at the top of the Sierra de Gador (~1600 m; see location in Fig. 2)

366



367

368 **Figure 4.** AHe ages of the Sierra de Gador plotted against effective uranium (eU) content. The
 369 ‘true’ AHe age (9.2 ± 0.7 Ma) corresponds to the AHe age associated with the grain showing
 370 the highest eU content (see text for explanation). AFT ages from this study (Ga-04) and
 371 published data (PB365 and PB367 from Platt *et al.*, 2005) are also reported for comparison.
 372 Inset shows all of the LT-thermochronological data on an age-elevation profile



373

374 **Figure 5.** Exhumation story and landscape evolution of the Sierra de Gador domain during
 375 Neogene times. (A) Neogene cooling path obtained from inverse modelling: thick black line =
 376 expected model; thin black lines = the 95% confidence interval. Inset shows the comparison
 377 between the Sierra de Gador cooling path (black line) and the Sierra Nevada cooling paths
 378 published by Vázquez *et al.* (2011) (light and dark grey lines). (B) Sketch showing the main
 379 stages of tectonic and landscape evolution of the Sierra de Gador-Sierra Nevada domain
 380 (deduced from LT thermochronological data and geological constraints).

